Title

Amyloid β-Protein Assembly and Alzheimer's Disease: Dodecamers of Aβ42, but Not of Aβ40, Seed Fibril Formation

Journal

Journal of the American Chemical Society, 138(6)

ISSN

0002-7863

Authors

Economou, Nicholas J
Giammona, Maxwell J
D., Thanh
et al.

Publication Date

2016-02-17

DOI

10.1021/jacs.5b11913

Peer reviewed

JACS
JOURNAL OF THE AMERICAN CHEMICAL SOCIETY
Communication
pubs.acs.org/JACS

Amyloid β-Protein Assembly and Alzheimer's Disease: Dodecamers of Aβ42, but Not of Aβ40, Seed Fibril Formation

Nicholas J. Economou,[†,§] Maxwell J. Giammona,[†,§] Thanh D. Do,[†] Xueyun Zheng,[†] David B. Teplow,[‡] Steven K. Buratto,[*,†] and Michael T. Bowers[*,†]

[†]Department of Chemistry and Biochemistry, University of California, Santa Barbara, California 93106, United States

[‡]Department of Neurology, David Geffen School of Medicine at UCLA; Mary S. Easton Center for Alzheimer's Disease Research at UCLA; and Brain Research Institute and Molecular Biology Institute, University of California, 635 Charles Young Drive South, Los Angeles, California 90095, United States

Supporting Information

ABSTRACT: Evidence suggests that oligomers of the 42-residue form of the amyloid β-protein (Aβ), Aβ42, play a critical role in the etiology of Alzheimer's disease (AD). Here we use high resolution atomic force microscopy to directly image populations of small oligomers of Aβ42 that occur at the earliest stages of aggregation. We observe features that can be attributed to a monomer and to relatively small oligomers, including dimers, hexamers, and dodecamers. We discovered that Aβ42 hexamers and dodecamers quickly become the dominant oligomers after peptide solubilization, even at low (1 μM) concentrations and short (5 min) incubation times. Soon after (≥10 min), dodecamers are observed to seed the formation of extended, linear preprotofibrillar β-sheet structures. The preprotofibrils are a single Aβ42 layer in height and can extend several hundred nanometers in length. To our knowledge this is the first report of structures of this type. In each instance the preprotofibril is associated off center with a single layer of a dodecamer. Protofibril formation continues at longer times, but is accompanied by the formation of large, globular aggregates. Aβ40, by contrast, does not significantly form the hexamer or dodecamer but instead produces a mixture of smaller oligomers. These species lead to the formation of a branched chain-like network rather than discrete structures.

The amyloid β-protein (Aβ) is thought to play a seminal role in Alzheimer's disease (AD).[1] Aβ is produced by serial endoproteolytic cleavage of the amyloid precursor protein, a type I transmembrane protein. These cleavages give rise to various forms of Aβ that differ in length at their C-termini. The most abundant of these are 40 (Aβ40) or 42 (Aβ42) residues long (Scheme S1). Although the nominal concentration of Aβ40 in humans is approximately 10 times that of Aβ42, the latter peptide is most tightly linked to AD pathogenesis.[2] Early studies suggested that Aβ fibril formation was the seminal neuropathogenic event in AD.[3] For this reason, both Aβ40 and Aβ42 have been the subject of extensive studies of peptide aggregation.[4−6] However, recent evidence has shown that soluble oligomeric forms of Aβ now appear to be the most important effectors of the disease.[1,7−9] If so, the development of oligomerization inhibitors would be facilitated by a more rigorous understanding of the mechanisms by which initial Aβ dimerization, and higher-order oligomer assembly, occur.[10] The Aβ monomer has been shown by NMR to fold into a strand−loop−strand conformation stabilized by intramolecular β-strand interactions. This folded conformation appears to facilitate the formation of the extended β-sheets that form mature amyloid fibrils.[11−13] It has been suggested in AFM studies that small Aβ oligomers act as seeds that induce oligomerization of adjacent monomers, similar to the mechanism of template-mediated prion conversion.[6,14,15] Studies using ion-mobility based mass spectrometry (IMS-MS) have attempted to address exactly which types of oligomers are formed and whether these oligomers act as seeds for fibril growth.[16,17] These studies revealed that even order oligomers were dominant, 2, 4, 6, and 12 with high populations of hexamers and dodecomers.[17] The role played by these oligomers remains an open question, however. Understanding the amyloid initiation and growth mechanism in Aβ would be very helpful in identifying therapeutic targets for effective AD disease treatment. We address this point later in this Communication

Atomic Force Microscopy (AFM) is an effective tool for visualizing large Aβ structures such as fibrils[6,14,15,18−21] and can also be used to gain information on the mechanical properties of these structures.[22,23] Using AFM as a technique to image smaller structures such as monomers, dimers, and other small oligomers is highly desirable but carries with it significant challenges. The details of the AFM methods we use are given in the Supporting Information. AFM techniques by their nature have excellent vertical resolution, but their horizontal resolution is dependent on the geometry of the AFM tip. Folded Aβ monomers are extremely small (~2 nm in diameter),[24,25] which makes them difficult to resolve unless extremely sharp AFM tips are used. The Smith group at SUNY Stony Brook used super sharp tips to collect images of Aβ42 at early stages of aggregation.[6,26,27] They were able to distinguish various oligomers and to propose a model for how their growth occurs.[26] They theorize that β-sheet-like dimers can directly associate to form protofibrils which then go on to form fibrils. They also suggest oligomers with β-sheet content can be formed in a parallel pathway and these oligomers eventually

Received: November 13, 2015

DOI: 10.1021/jacs.5b11913
J. Am. Chem. Soc. XXXX, XXX, XXX−XXX

rearrange to form fibrils. However, certain aspects of the conclusions of this study do not agree well with other models for oligomer aggregation.[16,17,28] Here, we seek to obtain a more complete picture of the time dependence of the oligomer population in solution by altering the sample preparation technique.

Figure 1 shows representative AFM topography images of Aβ42 using super sharp tips at solution incubation times of 5 and 10 min. In all images shown here, the sample has been directly deposited on the mica surface without further treatment. We found rinsing the surface following deposition resulted in removal of a large fraction of deposited material making it impossible to follow structural evolution as incubation time increased. See SI for details. At 5 min, we see almost exclusively small circular aggregates with heights principally between 0.75 and 1.50 nm. We attribute these features to single (0.75 nm) or double (1.5 nm) layers of Aβ42. Most of these features have a circular profile consistent with previous AFM studies.[6,26,27] The observed diameters are 10 to 15 nm measured by the base width. Previous IMS-MS data show the dominant oligomers in solution under conditions similar to those used here are hexamers and dodecamers.[16,17] The cross sections reported for the hexamer and dodecamer structures agree well with the dimensions of the features in Figure 1A after tip deconvolution.[16,17] Hence, given the circular profile and the measured dimensions we assign the features in Figure 1 with heights under 1 nm as hexamers and those near 1.5 nm as dodecamers. We also see a very low density of structures at 2.25 and 3 nm heights. These are not predicted to be abundant based on mass spectrometry studies.[16,17] It is possible that these larger features correspond to amorphous aggregates of several smaller oligomers, as they often have a larger diameter (~25 nm) than the hexamer or dodecamer.

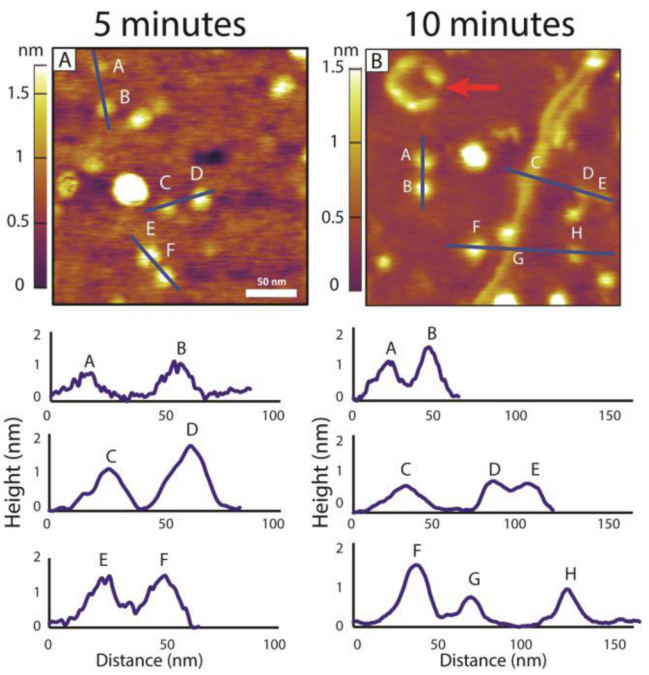

Figure 1. Representative AFM topography images of Aβ42 after (A) 5 and (B) 10 min of incubation in a 1 μM solution. Below each image are line cuts illustrating the heights of the observed features. (A) Features A, B, and C indicate Aβ hexamers, and D, E, and F indicate Aβ dodecamers consisting of two stacked hexamers. (B) shows that hexamers and dodecamers are still present after 10 min. Features C and G show a preprotofibril structure.

In the bottom half of Figure 1A are plotted line cuts through selected features in the image above giving the heights along the line. Features A, B, and C have heights less than 1 nm associated with single layer oligomers. We assign these features to hexamers. Features D, E, and F are approximately twice as high as A, B, and C, and hence we assign these features as dodecamers. There are no elongated, fibril-like features present at the 5 min incubation time.

Figure 1B is an image taken at a 10 min incubation time. Many of the 5 min features are still present, but new features are also evident. For example, in the upper left of Figure 1B is what appears to be 6 circular objects interacting with each other to form a quasi-circular construct (see arrow in Figure 1B). Height and width measurements indicate each of the 6 individual features are hexamers (data not shown). Such a feature is rare and does not increase in frequency with incubation time but does indicate there is a tendency for hexamers to interact with each other in this manner. Even more interesting is the appearance of a long, narrow filament-like structure in the right half of the image (over 200 nm long). Line cut height data (given below the image) indicate features B and F are dodecamers while A, D, E, and H are hexamers. The filament is 0.7 nm high (features C and G) and has an average width of approximately 10 nm. Given its physical characteristics we term this feature as a "pre-protofibril" and discuss it in more detail shortly.

Longer time images are given in Figure 2. By 20 min the density of preprotofibrils has grown considerably. The line cut E verifies these abundant species have heights of only 0.7 nm and widths of approximately 10 nm. Their lengths are clearly greater than 250 nm, as they extend beyond the image area in both directions. The larger spherical aggregates have also grown in frequency while the dodecamers and hexamers, although diminished in relative frequency, are still present (line cut A,B). These trends continue as evidenced by the 60 min image given in Figure 2B. Here clumping of the large spherical aggregates is clearly observed, consistent with earlier AFM studies taken at higher concentrations and longer incubation times.[26,27]

In summary we emphasize the *solution* evolution of the features observed in Figures 2 and 3. In all cases the solution spent approximately 2 min being vacuum-dried after being drop cast on the mica. As a consequence, the different structures observed are directly related to the incubation time in solution and not to surface−Aβ interactions. This point is more fully discussed in the Supporting Information.

A portion of the 10 min image is expanded and given as Figure 3A. There are two circular features shown as well as a portion of the preprotofibril. The left-most feature is feature F in Figure 1B and has been assigned as a dodecamer. The second circular feature is also a dodecamer, as determined by height and width measurements (data not shown). The most interesting and important aspect of this image is the fact the long preprotofibril appears to be growing out of the lower hexamer of the dodecamer. There has long been a view that Aβ fibrils were seeded by smaller structures, but until now there has been no direct evidence of the nature of the seed. There are essentially two limiting mechanisms that have been put forward for fibril growth in Aβ solutions.[1,27,29] The first one involves initial formation of a "seed" oligomer followed by monomer templating and addition to form β-sheet structured prefibrils that eventually become fibrils (the nucleated polymerization

DOI: 10.1021/jacs.5b11913
J. Am. Chem. Soc. XXXX, XXX, XXX−XXX

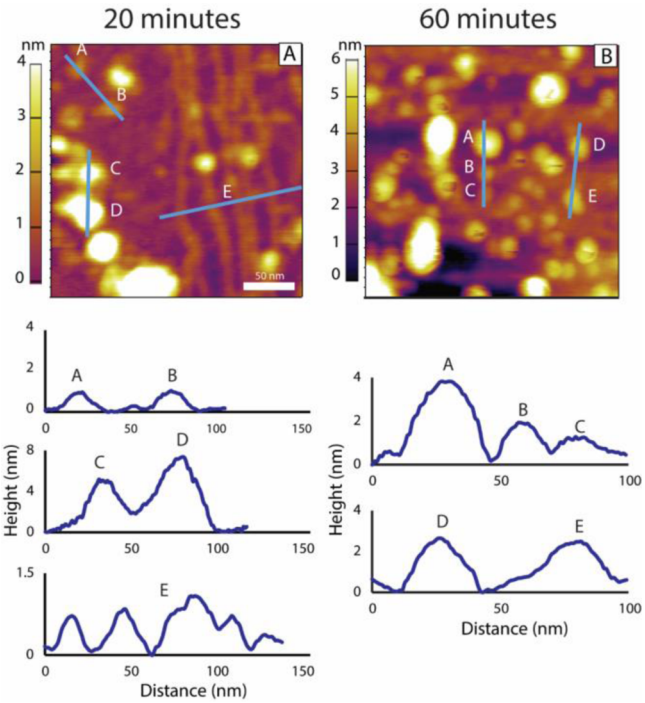

Figure 2. Representative AFM topography images of Aβ42 after (A) 20 and (B) 60 min of incubation in a 1 μM solution. Below each image are line cuts illustrating the heights of the observed features. (A) shows that after 20 min while dodecamers sized structures are still present (features A and B) a much higher density of larger globular aggregates has also formed (features C and D). Also present is a much larger amount of the preprotofibril structures shown by feature E. (B) shows that, after 60 min, large globular aggregates have come to dominate the morphology.

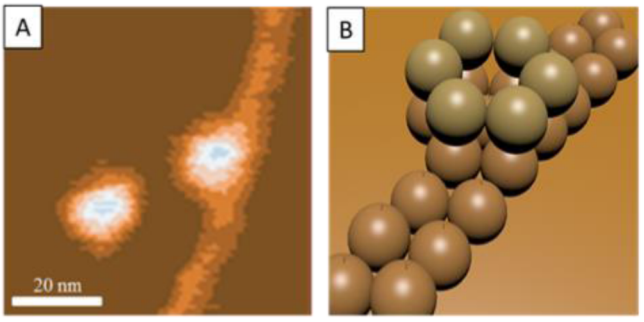

Figure 3. (A) Topographic image of Aβ42 cast from a 1 μM solution after 10 min of incubation showing the interaction between dodecamers and extended preprotofibrils. (B) Schematic cartoon of this growth mechanism.

mechanism).[30] The second involves Aβ oligomer condensation to form protofibrils directly (the nucleated conformational conversion pathway).[31] In this latter pathway it is ambiguous how and when β-sheet based structures are formed.

In a time sequence, dodecamers appear early on and then later in time filaments appear and are always associated with dodecamers (Figures 1 and 3). Hence the data strongly implicate the dodecamers as the seeds for the earliest fibril formation. These preprotofibrils have all of the physical characteristics of the β-sheet structures found experimentally in Aβ42 fibrils.[32] This is, to our knowledge, the first direct observation of the connection between known Aβ42 assemblies (hexamers and dodecamers) and the fibrils themselves.[16,17] This observation unambiguously shows the dodecamer as "on pathway" for fibril formation, an unanswered question up to this point. There has previously been evidence that the dodecamer is a likely proximate toxic agent in transgenic mice studies.[33] Hence there must be a delicate interplay between the dodecamer acting as the toxic agent in AD and its tendency to seed fibril formation. The latter process produces insoluble aggregates that are less toxic than the oligomers and may actually be protective.[34] The Aβ42 dodecamer is emerging as the central player in the molecular basis for Alzheimer's disease.

The dominant alloform of the Aβ-protein in vivo is Aβ40, typically making up 90% of the Aβ-protein present.[2] Previous studies have indicated that Aβ40 forms fibrils more slowly than Aβ42 and by a different mechanism.[35,36] IMS-MS experiments unambiguously showed Aβ40 forms tetramers as the terminal oligomer species while Aβ42 formed dodecamers as the terminal oligomer species.[16,17] Our AFM results for Aβ40 are summarized in Figure 4.

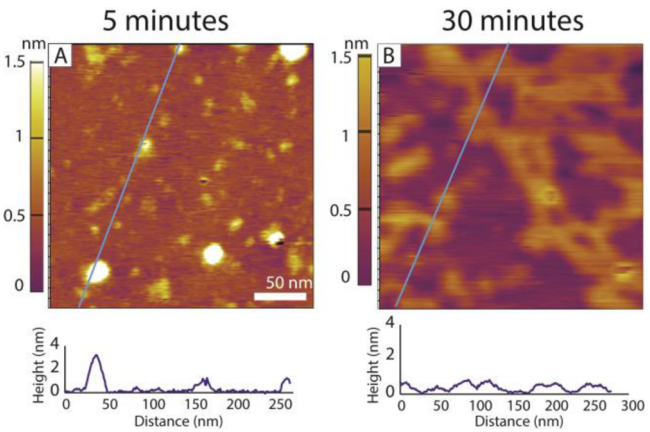

Figure 4. Representative AFM topography images of Aβ40 incubated after (A) 5 and (B) 30 min of incubation in a 1 μM solution. Below each image is a line cut to illustrate the height of the features present. In (A) the morphology is dominated by much smaller features than were observed at this time for Aβ42. (B) shows a peptide film of constant height that deposited onto the surface suggesting that most of the protein remains in the monomer or other low order oligomer state, weakly associated in solution.

Figure 4A shows a low density of spherical features. The mica surface is coated with monomers and very small oligomers (dimers and tetramers) with the occasional larger spherical aggregate as shown by the line cut below the image. At longer incubation times the few spherical aggregates diminish in frequency as shown in the 30 min image in Figure 4B. This image is dominated by a highly branched network of chain-like segments 1 nm or less in height and 10 nm in width on average, suggesting the network is β-sheet in character.[32] This network continues to develop at longer times until monomer and small oligomers are no longer available (data not shown). At no time frame (5 to 60 min) do we observe long single preprotofibrils in any of the Aβ40 images, nor do we observe the onset of any portion of this branched network with a specific oligomer as was observed for Aβ42 (Figure 3). These results are fully consistent with earlier ion mobility studies where oligomer formation in Aβ40 terminated at the tetramer.[16] They also correlate with the fact that Aβ40 is much less toxic than Aβ42 and that oligomers of Aβ40 were not observed in transgenic

DOI: 10.1021/jacs.5b11913
J. Am. Chem. Soc. XXXX, XXX, XXX−XXX

mice studies while those of Aβ42 were observed.[33,34] In addition it has been observed that hetero-oligomers of Aβ40 and Aβ42 terminate at the tetramer which suggests that Aβ40 is cyto-protective rather than cyto-toxic.[37]

In summary, we have used high resolution atomic force microscopy to probe the earliest stages of Aβ aggregation. We have shown direct evidence that Aβ42 undergoes rapid formation of hexamers and dodecamers with the dodecamers seeding the formation of extended preprotofibrils. Larger globular structures form at longer incubation times. Aβ40, on the other hand, undergoes a different assembly mechanism where hexamers and dodecamers are not involved resulting in the formation of what appear to be branched β-sheet structures and a much lower frequency of large globular aggregates. These results are fully consistent with earlier data from IMS-MS and other methods and give molecular insight into why Aβ42 is the central player in the molecular basis of Alzheimer's disease and why Aβ40 is not.

■ ASSOCIATED CONTENT

Supporting Information

The Supporting Information is available free of charge on the ACS Publications website at DOI: 10.1021/jacs.5b11913.

Included are the AFM methodology used, sample preparation techniques, images comparing the rinse and no rinse sample preparations methods, larger scale (5 μM) images of Aβ42 at each incubation time and Aβ40 after 30 min (PDF)

■ AUTHOR INFORMATION

Corresponding Authors

*buratto@chem.ucsb.edu

*bowers@chem.ucsb.edu

Author Contributions

§N.J.E. and M.J.G. contributed equally.

Notes

The authors declare no competing financial interest.

■ ACKNOWLEDGMENTS

We are grateful to acknowledge the support of the National Institute of Health Grant Number 1R01AG047116-01 (M.T.B.).

■ REFERENCES

(1) Roychaudhuri, R.; Yang, M.; Hoshi, M. M.; Teplow, D. B. *J. Biol. Chem.* **2009**, *284*, 4749.

(2) Younkin, S. G. *Ann. Neurol.* **1995**, *37*, 287.

(3) Hardy, J.; Higgins, G. *Science* **1992**, *256*, 184.

(4) Snyder, S.; Ladror, U.; Wade, W.; Wang, G.; Barrett, L.; Matayoshi, E.; Huffaker, H.; Krafft, G.; Holzman, T. *Biophys. J.* **1994**, *67*, 1216.

(5) Goldsbury, C. S.; Wirtz, S.; Müller, S. A.; Sunderji, S.; Wicki, P.; Aebi, U.; Frey, P. *J. Struct. Biol.* **2000**, *130*, 217.

(6) Ahmed, M.; Davis, J.; Aucoin, D.; Sato, T.; Ahuja, S.; Aimoto, S.; Elliott, J. I.; Van Nostrand, W. E.; Smith, S. O. *Nat. Struct. Mol. Biol.* **2010**, *17*, 561.

(7) Harper, J. D.; Wong, S. S.; Lieber, C. M.; Lansbury, P. T., Jr *Chem. Biol.* **1997**, *4*, 119.

(8) Bernhardt, N. A.; Berhanu, W. M.; Hansmann, U. H. E. *J. Phys. Chem. B* **2013**, *117*, 16076.

(9) Demuro, A.; Mina, E.; Kayed, R.; Milton, S. C.; Parker, I.; Glabe, C. G. *J. Biol. Chem.* **2005**, *280*, 17294.

(10) Teplow, D. B. *Alzheimer's Res. Ther.* **2013**, *5*, 39.

(11) Hou, L. M.; Shao, H. Y.; Zhang, Y. B.; Li, H.; Menon, N. K.; Neuhaus, E. B.; Brewer, J. M.; Byeon, I. J. L.; Ray, D. G.; Vitek, M. P.; Iwashita, T.; Makula, R. A.; Przybyla, A. B.; Zagorski, M. G. *J. Am. Chem. Soc.* **2004**, *126*, 1992.

(12) Sticht, H.; Bayer, P.; Willbold, D.; Dames, S.; Hilbich, C.; Beyreuther, K.; Frank, R. W.; Rosch, P. *Eur. J. Biochem.* **1995**, *233*, 293.

(13) Vivekanandan, S.; Brender, J. R.; Lee, S. Y.; Ramamoorthy, A. *Biochem. Biophys. Res. Commun.* **2011**, *411*, 312.

(14) Harper, J. D.; Lieber, C. M.; Lansbury, P. T., Jr *Chem. Biol.* **1997**, *4*, 951.

(15) Serem, W. K.; Bett, C. K.; Ngunjiri, J. N.; Garno, J. C. *Microsc. Res. Tech.* **2011**, *74*, 699.

(16) Bernstein, S. L.; Dupuis, N. F.; Lazo, N. D.; Wyttenbach, T.; Condron, M. M.; Bitan, G.; Teplow, D. B.; Shea, J.-E.; Ruotolo, B. T.; Robinson, C. V.; Bowers, M. T. *Nat. Chem.* **2009**, *1*, 326.

(17) Bernstein, S. L.; Wyttenbach, T.; Baumketner, A.; Shea, J.-E.; Bitan, G.; Teplow, D. B. *J. Am. Chem. Soc.* **2005**, *127*, 2075.

(18) Parbhu, A.; Lin, H.; Thimm, J.; Lal, R. *Peptides* **2002**, *23*, 1265.

(19) Qiang, W.; Kelley, K.; Tycko, R. *J. Am. Chem. Soc.* **2013**, *135*, 6860.

(20) Zhou, X.; Zhang, Y.; Zhang, F.; Pillai, S.; Liu, J.; Li, R.; Dai, B.; Li, B.; Zhang, Y. *Nanoscale* **2013**, *5*, 4816.

(21) Stine, W. B.; Snyder, S. W.; Ladror, U. S.; Wade, W. S.; Miller, M. F.; Perun, T. J.; Holzman, T. F.; Krafft, G. A. *J. Protein Chem.* **1996**, *15*, 193.

(22) Raman, E. P.; Takeda, T.; Barsegov, V.; Klimov, D. K. *J. Mol. Biol.* **2007**, *373*, 785.

(23) Hane, F. T.; Lee, B. Y.; Petoyan, A.; Rauk, A.; Leonenko, Z. *Biosens. Bioelectron.* **2014**, *54*, 492.

(24) Losic, D.; Martin, L. L.; Mechler, A.; Aguilar, M. I.; Small, D. H. *J. Struct. Biol.* **2006**, *155*, 104.

(25) Baumketner, A.; Bernstein, S. L.; Wyttenbach, T.; Bitan, G.; Teplow, D. B.; Bowers, M. T.; Shea, J.-E. *Protein Sci.* **2006**, *15*, 420.

(26) Mastrangelo, I. A.; Ahmed, M.; Sato, T.; Liu, W.; Wang, C.; Hough, P.; Smith, S. O. *J. Mol. Biol.* **2006**, *358*, 106.

(27) Fu, Z.; Aucoin, D.; Davis, J.; Van Nostrand, W. E.; Smith, S. O. *Biochemistry* **2015**, *54*, 4197.

(28) Bleiholder, C.; Dupuis, N. F.; Wyttenbach, T.; Bowers, M. T. *Nat. Chem.* **2011**, *3*, 172.

(29) Cohen, S. I. A.; Linse, S.; Luheshi, L. M.; Hellstrand, E.; White, D. A.; Rajah, L.; Otzen, D. E.; Vendruscolo, M.; Dobson, C. M.; Knowles, T. P. J. *Proc. Natl. Acad. Sci. U. S. A.* **2013**, *110*, 9758.

(30) Harper, J. D.; Lansbury, P. T. *Annu. Rev. Biochem.* **1997**, *66*, 385.

(31) Serio, T. R.; Cashikar, A. G.; Kowal, A. S.; Sawicki, G. J.; Moslehi, J. J.; Serpell, L.; Arnsdorf, M. F.; Lindquist, S. L. *Science* **2000**, *289*, 1317.

(32) Walsh, D. M.; Lomakin, A.; Benedek, G. B.; Condron, M. M.; Teplow, D. B. *J. Biol. Chem.* **1997**, *272*, 22364.

(33) Lesné, S.; Koh, M. T.; Kotilinek, L.; Kayed, R.; Glabe, C. G.; Yang, A.; Gallagher, M.; Ashe, K. H. *Nature* **2006**, *440*, 352.

(34) Cheng, I. H.; Scearce-Levie, K.; Legleiter, J.; Palop, J. J.; Gerstein, H.; Bien-Ly, N.; Puoliväli, J.; Lesné, S.; Ashe, K. H.; Muchowski, P. J.; Mucke, L. *J. Biol. Chem.* **2007**, *282*, 23818.

(35) Bitan, G.; Kirkitadze, M. D.; Lomakin, A.; Vollers, S. S.; Benedek, G. B.; Teplow, D. B. *Proc. Natl. Acad. Sci. U. S. A.* **2003**, *100*, 330.

(36) Roychaudhuri, R.; Yang, M.; Deshpande, A.; Cole, G. M.; Frautschy, S.; Lomakin, A.; Benedek, G. B.; Teplow, D. B. *J. Mol. Biol.* **2013**, *425*, 292.

(37) Murray, M. M.; Bernstein, S. L.; Nyugen, V.; Condron, M. M.; Teplow, D. B.; Bowers, M. T. *J. Am. Chem. Soc.* **2009**, *131*, 6316.

DOI: 10.1021/jacs.5b11913
J. Am. Chem. Soc. XXXX, XXX, XXX−XXX

Supporting Information

Amyloid β-protein assembly and Alzheimer's disease: Dodecamers of Aβ42, but not of Aβ40, seed fibril formation

Nicholas J. Economou[‡], Maxwell J. Giammona[‡], Thanh D. Do, Xueyun Zheng, David B. Teplow[†], Steven K. Buratto*, Michael T. Bowers*

Department of Chemistry and Biochemistry, University of California, Santa Barbara, California 93106, United States

[†]Department of Neurology, David Geffen School of Medicine at UCLA; Mary S. Easton Center for Alzheimer's Disease Research at UCLA; and Brain Research Institute and Molecular Biology Institute, University of California, 635 Charles Young Drive South, Los Angeles, California 90095, United States.

[‡]These authors contributed equally.

AFM Methods

The AFM experiments were conducted in tapping mode in air on an Asylum MFP-3D instrument. To maximize lateral resolution, we employed a super sharp silicon AFM probe (Nanoworld SSS-NCT) with a nominal spring constant of 40 N/m. Optimization of imaging conditions included using a low drive amplitude to minimize contact forces and using careful tip engage procedures.

Sample Preparation

Samples were prepared by dissolving Aβ in hexafluoroisopropanol (Sigma-Aldrich, St. Louis) and then evaporating the solvent to create a peptide film. This film was then re-dissolved in a 10 mM ammonium acetate buffer solution, pH 7.4, to achieve a final Aβ concentration of 1μM. This solution was incubated at room temperature. A 100μL aliquot was then periodically removed and deposited onto a freshly cleaved piece of mica (TedPella, highest grade disks) and dried in a vacuum desiccator. We did not rinse the mica substrate at any time post-deposition. We observed that rinsing the disk before imaging resulted in removal of a large fraction of the deposited material (Figure S1) making it impossible to follow the actual solution phase growth processes. Deposition of the protein onto the mica in many areas completely covered the substrate (Figures S2 and S3). For this reason, in order to image small oligomers on mica rather than on top of other protein structures, areas of the sample were selected for imaging that had a lower density of protein. We found that complete evaporation of the solvent required about 2 min, hence the total aggregation time was determined by adding 2 min to the incubation time. We noticed very little difference in aggregation behavior after one hour, indicating that the self-aggregation process proceeds quickly and reaches a relatively stable state (data not shown).

On the possibility of surface mediated protein growth

Others have shown that under certain conditions that for either Aβ42[1] or for a fragment of this peptide[2] the surface can play a role in determining the structure of oligomers and/or fibrils that are formed. While the conditions for these experiments[1,2] are very different from those we use here, it was important for us to insure we were observing solution assembly of the peptides and not surface assembly. Hence we chose to use small concentrations of peptide (1 μM) in water/buffer in order to

minimize or eliminate effects due to solvent. Further we carefully surveyed the entire surface covered by the droplet on the mica. We noticed, especially at longer incubation times, that some assemblies adhered on top of (or very near) other assemblies and hence we chose other areas of the surface for detailed study that were free from this complication. In this way we were able to insure that all structures of interest were in direct contact with the mica surface and that the structural parameters we measured accurately reflected the assembly of interest. Multiple experiments were done at each incubation time and in all cases equivalent results were obtained. Of paramount importance is the fact that changes in the distribution of structures observed correlated only with solution incubation time, a result that unambiguously indicates that solution assembly was being observed. At higher concentrations we sometimes observed product condensation "rings" on the edges of the droplet but these were very large (10's of microns). This process was not observed in any of the 1μM experiments reported in this paper.

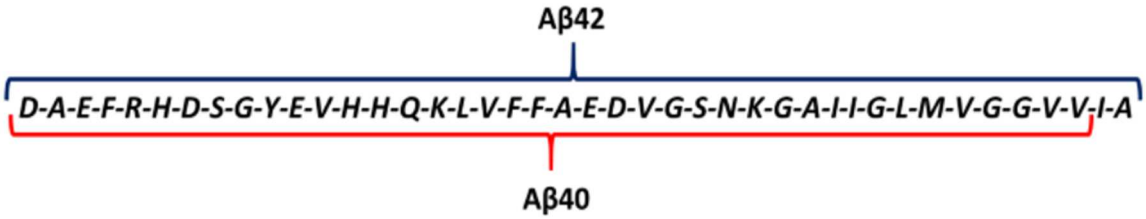

Scheme S1: Primary Structure of Aβ42, blue line, and Aβ40, red line, with the N-terminus at the left

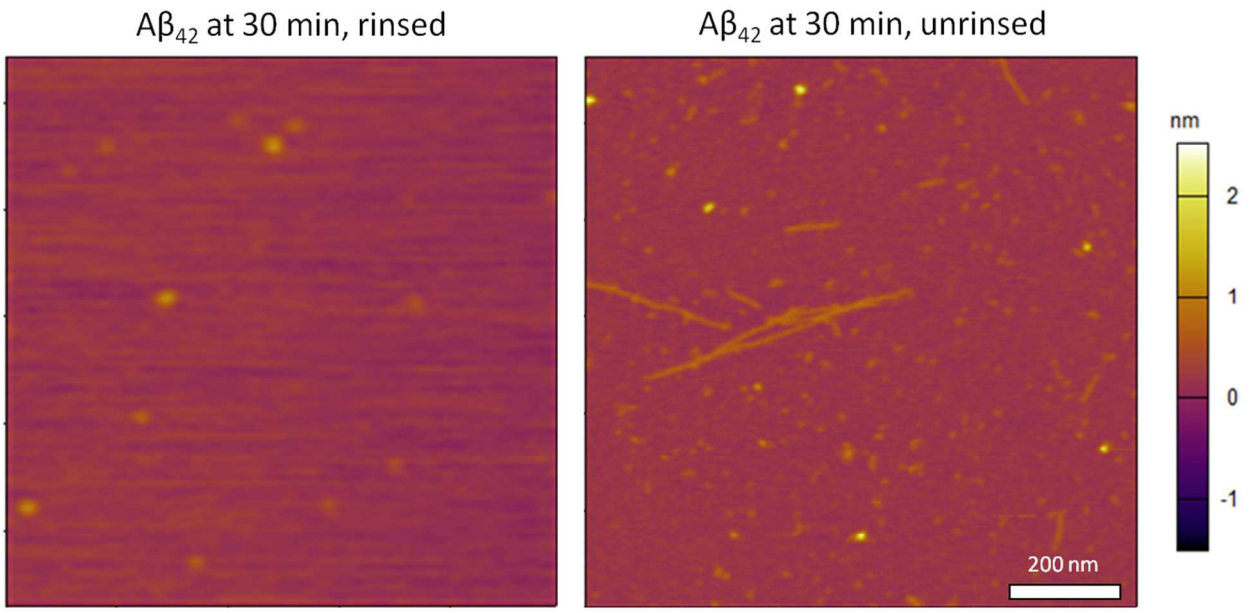

Figure S1: Comparison of Aβ42 on mica after a 30 minute incubation period. In the left image the mica was lightly rinsed following the deposition of sample onto the surface whereas in the right image, the sample was left to dry without a rinsing step.

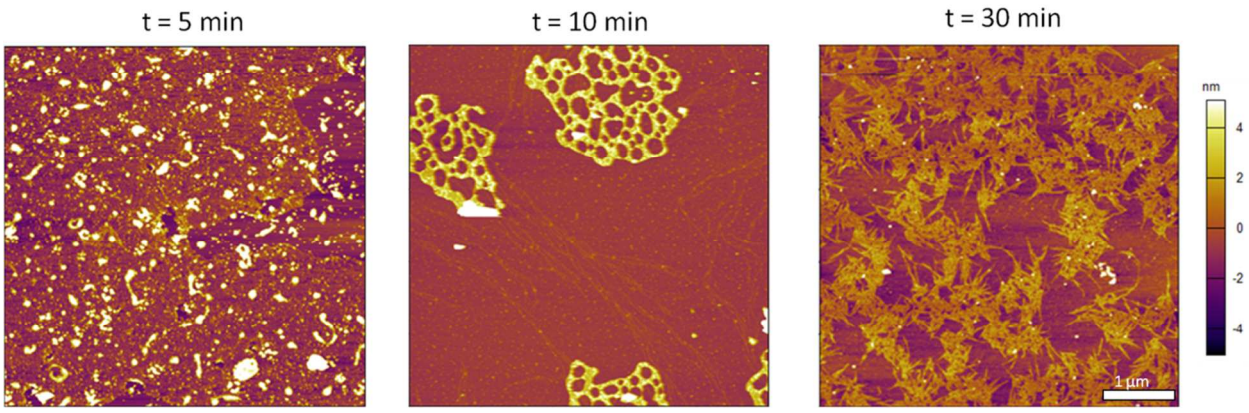

Figure S2: Larger scale (5µm) images of $A\beta_{42}$ growth for samples incubated for 5, 10, and 30 minutes.

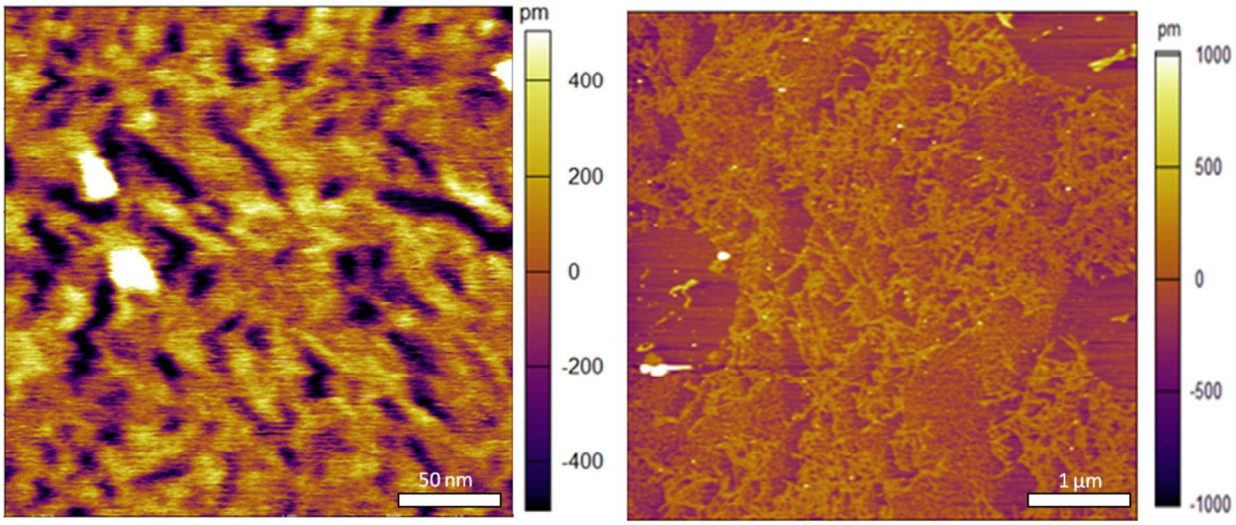

Figure S3: Film of $A\beta_{40}$ incubated for 30 min and imaged at different length scales: 250nm (left) and 5 µm (right)

Supplemental References

1. Shen, L.; Adache, T.; Vander Bout, D.; Zhu, X-Y. *J. Am. Chem. Soc.* **2012**, *134*, 14172.

2. Lin, Y-C.; Peterson, E. J.; Fakhraai, Z. *ACS Nano* **2014**, *8*, 10178.